IEEE Access
Multidisciplinary ⋮ Rapid Review ⋮ Open Access Journal

Received 17 November 2025, accepted 11 December 2025, date of publication 22 December 2025,
date of current version 31 December 2025.

Digital Object Identifier 10.1109/ACCESS.2025.3646849

APPLIED RESEARCH

Sliding Mode Control as an Efficient Method of Synchronization of High-Stability Oscillators With 1-pps Signals

PAWEŁ KUBCZAK, MIECZYSŁAW JESSA, AND JAKUB NIKONOWICZ, (Senior Member, IEEE)
Poznań University of Technology, 61-131 Poznań, Poland

Corresponding author: Paweł Kubczak (pawel.kubczak@put.poznan.pl)

This work was supported by the Polish Ministry of Science and Higher Education.

ABSTRACT Clock steering with a one pulse per second (1 PPS) signal is crucial for many modern telecommunication systems to provide high-performance time and frequency signals. In most telecom applications, the reference 1 PPS signal originates from an external source, typically the Global Navigation Satellite System (GNSS). Signals from GNSS are noisy, not always stationary, and can be disturbed intentionally or unintentionally by the operation of other devices, systems, or malicious attacks. In this paper, we propose the use of the Sliding Mode Control (SMC) algorithm for frequency and phase synchronization of a local oscillator, which has not been considered in telecommunications applications so far. The significance of our research lies in its ability to provide a practical and computationally efficient solution to oscillator synchronization, overcoming the complexity and high theoretical demands associated with existing optimal control techniques for high-stability oscillators. The effectiveness of the proposed algorithm was demonstrated for three types of generators used in telecommunication systems.

INDEX TERMS Synchronization of telecom devices, optimal control, GNSS, 1 PPS.

I. INTRODUCTION

Synchronizing the frequency and phase of high-stability oscillators with a one pulse per second (1 PPS) signal from an external source, typically from Global Navigation Satellite Systems (GNSS), is essential in various scientific and technological fields. The available literature on algorithms for synchronizing the frequency and phase of local oscillators is extensive. An overview of existing solutions are included in [1], [2], [3], [4]. The latest solutions utilize methods derived from the theory of optimal control [5] for phase and frequency synchronization of a local generator [1], [6], [7], [8], [9]. The main advantage of these methods is the high quality of phase and frequency tracking of the input signal by the local generator, as well as the short time required to enter synchronization. As noted in [4], particularly good results are achieved by using the Sliding Mode Control (SMC) algorithm to reduce the initial phase error quickly, and then switching to the algorithm using a Linear Quadratic Regulator (LQR) or Model Predictive Control (MPC). Although the LQR and MPC offer a higher quality of tracking than the SMC, they are significantly more complex than the SMC and need more time to reduce the initial error below the assumed value.

The primary objective of this paper is to validate the concept of utility of the SMC as an alternative to the LQR and MPC, which can also meet basic telecom standards, such as PRTC-B, for high-stability oscillators synchronized with 1 PPS signals.

Sliding Mode Control [10], [11], [12], [13], [14], [15] is a nonlinear control method characterized by its robustness to system uncertainties, external disturbances, and stability [10]. Its structure and control scheme are relatively simple, which facilitates straightforward implementation and tuning. A key advantage of SMC is its ability to provide a fast dynamic response, making it well-suited for systems that require rapid corrective actions. However, a known drawback of

The associate editor coordinating the review of this manuscript and approving it for publication was Ajit Khosla.

this approach is the phenomenon of chattering—undesirable high-frequency oscillations that may occur near the sliding surface—potentially affecting system stability and performance in sensitive applications. To minimize this effect, the Higher-Order Sliding Mode Control (HOSM) with a variable step was proposed, which, instead of forcing the sliding variable to zero, aims to drive this variable and its first derivative to zero.

This study demonstrates that for many telecom applications involving high-stability oscillators synchronized to an external 1 PPS source (including GNSS), SMC presents a viable standalone solution, which does not require switching to another algorithm. Crucially, the phase error and relative frequency accuracy of the local oscillator achieved with SMC do not significantly degrade compared to results obtained with more complex algorithms proposed in prior work [1], [4], and [9]. Furthermore, the requirements for Maximum Time Interval Error (MTIE) and Time Deviation (TDEV) for the Primary Reference Time Clock (PRTC) [16] can still be met. This is accomplished by introducing specific, uncomplicated additional operations within the SMC framework. These operations effectively reduce the magnitude of control voltage jumps, thereby minimizing the chattering effect during the sliding phase. A significant benefit of chatter reduction is the improved ability of the system to transition smoothly into a holdover state. Consequently, the proposed SMC approach offers an efficient alternative to significantly more complex frequency and phase synchronization techniques for high-stability oscillators, such as those based on LQR or MPC algorithms. In SMC, the control output is typically calculated using a simple, explicit algebraic equation. This involves only a few arithmetic operations per control cycle. In LQR, the control law is a state-feedback gain matrix multiplication. While still computationally fast, it involves vector-matrix multiplication, which is more intensive than the SMC equation, especially as the number of states increases. In MPC, this is the most demanding. At each time step, MPC requires solving a constrained optimization problem over a future horizon. Comparizon is shown in Table 1.

TABLE 1. Algorithms computational complexity.

Controller	Computational Task	Complexity
SMC [17]	Apply the signum function	O(n)
LQR [18]	Matrix-vector multiplication	$O(n^2)$
MPC [19]	Solve a constrained quadratic problem (iterative)	$O(p^3N^3)$ p, N horizon vars

The second section describes the model used and the SMC algorithm. The third section describes the implementation of the algorithm, including graphs of the MTIE and TDEV values obtained during the frequency and phase control of three types of highly stable generators, as well as a description of the algorithm for entering the holdover state in the absence of access to synchronization pulses. The paper ends with the conclusions and summary in section four.

II. THE MODEL

Figure 1 shows a block diagram illustrating the control loop model of a local high-stability voltage-controlled oscillator (VCO). This model is similar to that presented in [4].

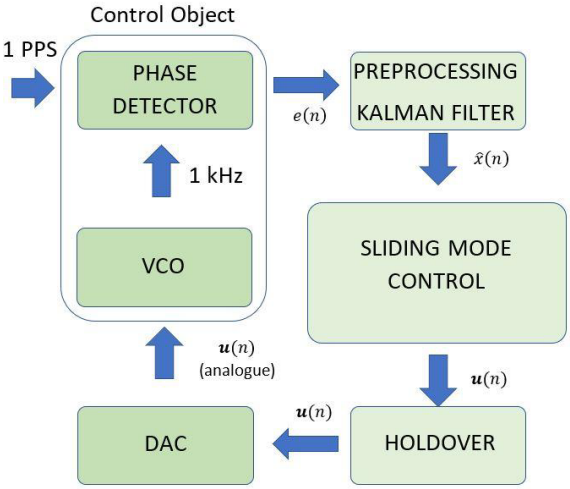

FIGURE 1. Block diagram illustrating the frequency and phase control of a local VCO with the sliding mode control algorithm.

The system receives a 1 PPS signal, which is used as the primary synchronization reference. Our analysis assumes that this signal is primarily affected by white frequency noise, which dominates over the considered time scales. Other noise types, such as random walk frequency noise, are treated as negligible in this context [20], [21].

The PHASE DETECTOR compares the phase of the incoming 1 PPS signal with the phase of the signal generated by the VCO. This comparison is performed cycle-by-cycle, with each measurement starting at the rising edge of the 1 PPS signal. The resulting phase difference is used to track and correct deviations in the oscillator's output.

In the PREPROCESSING block, phase measurement results are analyzed, considering the statistical properties of the 1 PPS signal and events that may affect those statistics, such as jamming or spoofing. Let us notice that the SMC considered in this paper, by itself, cannot distinguish between a valid signal and a spoofed or jammed one. If the spoofer introduces a smoothly varying, false trajectory, the SMC will diligently and correctly track this false trajectory. This is not a failure of the SMC algorithm itself, but a failure of the input data's integrity. A more detailed discussion of preprocessing can be found in [4], [22], and [23]. The preprocessing consists of three main steps:

1. *Initial phase reset*—To minimize the initial phase error, one of the first available 1 PPS pulses is used to reset the output of the frequency synthesizer or frequency divider, which generates a 1 kHz signal within the

feedback loop. This step is executed only once, upon signal acquisition.

2. *Outlier rejection*—Phase values that significantly deviate from the trend observed over the last $K>1$ samples are excluded using a median filter. This step removes anomalous measurements that could distort the estimation process.
3. *Kalman filtering* – A discrete Kalman filter is applied to reduce the impact of measurement noise and improve the stability of the phase estimates used in subsequent control.

The output of the preprocessing stage consists of filtered phase measurements, cleaned of outliers and smoothed to suppress noise effects.

The block labeled SLIDING MODE CONTROL implements a control strategy that ensures the system reaches and maintains synchronism at the current and over successive iterations. In this context, synchronism refers to the phase alignment between the locally generated signal and the filtered 1 PPS reference, with the additional requirement that the absolute phase error remains constrained within a defined tolerance.

In scenarios where the 1 PPS signal is temporarily unavailable, the HOLDOVER block refines the control word produced initially by the SMC algorithm. It aims to limit the initial relative frequency error, denoted as δf, during free-running operation. The final control signal is applied to a 20-bit digital-to-analog converter (DAC1220), whose output voltage determines the tuning of the VCO, thereby setting the system's output frequency in the absence of external synchronization.

The behavior of the system executing the control process shown in Figure 1 can be explained using the mathematical abstraction described in many books or journal papers, for example, in [4]. Because our goal is to minimize both the phase error $e(n)$ and relative frequency error δf, the state vector $\mathbf{x}(n)$ of the system shown in Figure 1 has two state variables:

$$\mathbf{x}(n) = \begin{bmatrix} x_{ph}(n) \\ x_{dph}(n) \end{bmatrix}, \tag{1}$$

where $x_{ph}(n)$ represents the phase offset of an object and $x_{dph}(n)$ is a derivative of $x_{ph}(n)$ describing the rate of change of the phase offset, thus representing the current frequency offset. The Kalman filter is an essential component of a control loop. A Kalman filter is the optimal solution when the measurements are distorted by white additive Gaussian noise [24]. Because this is also the case with the system in Figure 1, synchronized with a 1 PPS signal from GNSS, the choice of the Kalman filter as a tool for tuning the control algorithm seems obvious. In a Kalman filter, the process noise covariance and measurement noise covariance directly shape the Gaussian belief about the state. If these are wrong, the filter can become overconfident (too small a quotient of process noise covariance and measurement noise covariance) or too uncertain (too large a quotient of process noise covariance and measurement noise covariance), leading to divergence or poor estimation. A more detailed description of finding optimal Kalman filter parameters can be found in [22]. The robustness that makes SMC good at rejecting external physical disturbances also makes it good at rejecting wrong information from an imperfect state estimator. To conclude, if the Kalman filter becomes overconfident, the whole system with SMC will remain stable, but it will follow a wrong prediction of the phase. If Kalman becomes too uncertain, noise reduction will be lower; however, the system remains stable due to the properties of SMC [10]. The result of Kalman filtration is an estimate of $\mathbf{x}(n)$

$$\hat{x}(n) = \begin{bmatrix} \hat{x}_{ph}(n) \\ \hat{x}_{dph}(n) \end{bmatrix} \tag{2}$$

of the object state. The method for computing $\hat{x}(n)$ was described in detail in [4].

The objective of the control is to achieve a phase synchronization state as quickly as possible, and once achieved, to ensure that the relative frequency error δf is minimized. This enables the control system to transition to the holdover state with the least initial error after a 1 PPS signal is lost. According to the control theory, sliding control is the quickest method to reach the desired control plane position, [25], [26].

The control law is defined as follows:

$$\begin{cases} \hat{x}_{ph}(n) + \hat{x}_{dph}(n) > 0 \Rightarrow u(n) = \max u \\ \hat{x}_{ph}(n) + \hat{x}_{dph}(n) < 0 \Rightarrow u(n) = \min u \end{cases}, \tag{3}$$

where x_{ph} represents the phase offset of an object, x_{dph} is a derivative of x_{ph}, i.e., the frequency offset, $u(n)$ is the control voltage, and $\max u > \min u \geq 0$. If the total phase error and its rate of change are positive, the control receives the maximum voltage to rapidly decrease the phase error. Conversely, if the total voltage is negative, a minimum voltage is applied.

Note that the sliding control implemented in the system shown in Figure 1 is limited by the frequency tuning range of the VCO, period T, phase difference measurement, and user-defined value of $\Delta\varphi$ expressed in time units. Achieving a phase offset reduction to $\Delta\varphi$, regardless of the initial phase difference, is only possible with oscillators that have a relative frequency-tuning range below the specified threshold:

$$\delta f_{max} = \frac{\Delta f_{max}}{f_{nom}} = \Delta\varphi/T, \tag{4}$$

where Δf_{max} is the absolute value of the greatest detuning from the nominal frequency f_{nom} of oscillator VCO. For example, for $T = 1$ s and $\Delta\varphi = 10$ ns, the sliding control reduces the phase to value $\Delta\varphi$ only if the frequency-tuning range of the VCO does not exceed $\delta f_{max} = 10^{-8}$. In the case of a reduction of $\Delta\varphi$ to 1 ns, we have $\delta f_{max} = 10^{-9}$. The limitation given in (4) can be circumvented by introducing a scale factor s. If δf_{max} is s times the limit $\Delta\varphi/T$ and assuming the control voltage symmetric respect to zero, formulas (3) and (4) take the following form:

$$\begin{cases} \hat{x}_{ph}(n) + \hat{x}_{dph}(n) > 0 \Rightarrow u(n) = \max u/s(n) \\ \hat{x}_{ph}(n) + \hat{x}_{dph}(n) < 0 \Rightarrow u(n) = \min u/s(n) \end{cases}, \tag{5}$$

where the value of $s(n)$ is increased at a rate of $k \geq 1$ iterations, starting with $s(1)=1$ and ending with the value of s. This modification to the HOSM method reduces the chattering effect. The value of s depends on three parameters, δf_{max}, T, $\Delta\varphi$, and can be calculated by the fromula:

$$s \geq \left\lceil \frac{\delta f_{max}}{\delta\varphi} T \right\rceil, \tag{6}$$

where $\Delta\varphi > 0$ and $T > 0s$. For example, if $\delta f_{max} = \pm 2.2 \cdot 10^{-8}$, $\Delta\varphi = 10ns$ and $T = 1s$, we obtain $s = 3$. For the same δf_{max} and $\Delta\varphi$ but $T = 10$, it is that $s = 30$. Unfortunately, the rate of change in values s(n) and the nature of those changes that led to the fastest reduction of the initial phase difference to the value of $\Delta\varphi$ can only be determined experimentally. The cost is the greater time required to achieve phase synchronization with assumed accuracy $\Delta\varphi$. Note also that when scale factor s is applied, the range of the control voltage used in relation to the range offered by the VCO is reduced. To ensure the possibility of adjusting the VCO frequency over the entire available voltage range, which is necessary because of the aging processes occurring in the VCO and possible changes in the ambient parameters, predominantly the temperature, we propose the following modification of the control law (5):

$$\begin{cases} \hat{x}_{ph}(n) + \hat{x}_{dph}(n) > 0 \Rightarrow u(n) = h + (\max u - \min u)/2s(n) \\ \hat{x}_{ph}(n) + \hat{x}_{dph}(n) < 0 \Rightarrow u(n) = h - (\max u - \min u)/2s(n) \end{cases}, \tag{7}$$

where h is the voltage from the last holdover state. The initial value of h is equal to half of the voltage regulation range VCO, which can be both symmetric or asymmetric with respect to zero voltage. For example, for a voltage regulation range from 0 to 5 V ($\max u = 5\text{V}, \min u = 0\text{V}$) it will be $h = 2.5$ V. For $s = 5$, the available adjustment range is from 2 to 3 V. If the value *of h* for the last holdover state is, e.g., 3 V, then the available adjustment range will be from 2.5 V to 3.5 V. Note that with such a rule, the transition of the control system from time to time to the holdover state is advantageous, because it ensures frequency control over the entire range of VCO control voltages, regardless of the value of the s-factor but the control voltage limits cannot be greater than the maximum u and less than minimum u. Also note that *s,* calculated from formula (6), cannot be too large, as a large s results in a small range of frequency adjustment around the value corresponding to the last h. From the top, s limits the values of short-term frequency changes of the VCO used, which can be estimated by calculating the Allan deviation for an argument of no less than 100 seconds. This problem requires further theoretical and experimental studies. In this paper, we present the results for generators, for which this limitation does not matter, because the value of s was not greater than 5. Thus, the range of VCO frequency changes caused by voltage regulation around h was hundreds of times greater than the ADEV of the studied generators.

After reducing the phase difference to a value not exceeding $\Delta\varphi$, assumed by the user, the algorithm tracks the changed phases and frequency of the input 1 PPS signal. The problem arises when the control loses access to the 1 PPS signal and has to switch to the holdover state. The algorithm switches to the holdover state after missing at least 3 subsequent input impulses. In this state, further changes in the frequency and phase of the VCO output signal significantly depend on the last control word applied to the VCO input. Leaving the control word, resulting from formulas (5) and (7), would result in a significant initial frequency error in the holdover. Therefore, when a 1 PPS signal decay is detected, additional operations are performed in a block marked as HOLDOVER, the purpose of which is to replace the last word before the detection of the 1 PPS pulse decay with another word, guaranteeing a much smaller relative frequency error δf. A solution to this problem is a moving average filter (MAV), which determines the long-term trend and removes short-term fluctuations and noise [27]. Due to its recursive and running implementation, its complexity is constant and independent of the filter length. This makes the MAV filter exceptionally efficient, particularly for large window sizes, and is ideal for implementation in resource-constrained systems, such as microcontrollers. Noise reduction is proportional to the length of the filter and is approximately $\sqrt{K}$, where K is the number of averaged samples. The MAV filter is an essential solution used to determine the value of the code word after the loss of a 1 PPS signal. The initial value of the relative frequency error at the entry into the holdover state can be estimated using the formula:

$$\delta f_h \approx \frac{\Delta f_{osc}}{s\sqrt{K}}, \tag{8}$$

where Δf_{osc} is the frequency-tuning range of a given generator, s is the value of the divisor in (5) and (7), and K is the length of the MAV averaging filter. In practical applications, the range value describing the relative initial frequency offset in the holdover state, expressed as a percentage of the generator tuning range, is useful and takes the following form:

$$p_h = \frac{\Delta f_h}{\Delta f_{osc}} 100\% \approx \frac{1}{s\sqrt{K}} 100\%. \tag{9}$$

The value for K was determined empirically to achieve the value for p_h below 0.5%. During the holdover state, no prediction algorithm for frequency changes of the VCO was implemented. Predictive models, such as ARIMA (Autoregressive Integrated Moving Average) and Neural Networks (NNs), are designed to learn the underlying patterns and trends within a time series. Their primary function is to extrapolate the frequency trend into the future, actively counteracting the known drift during the holdover period. The function of MAV is to calculate the mean of the most recent control values over a set window. This provides a highly stable, low-noise estimate of the oscillator's current state by filtering out short-term fluctuations. It's computationally simple and sufficient for most applications to provide a stable

''last known good'' frequency value at the start of holdover. This minimizes the initial frequency error. In more complex systems, both approaches can be used: a MAV to provide a clean, noise-free starting point, and a predictive model to take over and manage the long-term drift. However, this extends the scope of this paper, which primarily focuses on the feasibility of using SMC for fast synchronization of a high-stability oscillator to meet telecom standards. Thus, the behavior of the oscillator phase was only determined by the VCO parameters in a free-running state and by the initial offset (8). The degradation over time is governed almost entirely by the oscillator's intrinsic characteristics, specifically systematic aging. Every crystal oscillator has a predictable long-term frequency drift, often measured in parts per billion (ppb) per day. This will cause a steady, often almost linear, drift in the frequency, and environmental sensitivity—the oscillator's frequency is highly sensitive to changes in ambient temperature. After detecting 3 or more subsequent input pulses, we exit the holdover state. The algorithm for returning from the holdover state was the same as for a ''cold'' start, i.e., the control was performed according to the modified control law described by (7), starting from the last stored control word (value for h) and $s = 1$.

III. IMPLEMENTATION OF THE SMC

The initial phase of the current implementation of the SMC algorithm is identical to that described in [4]. Since the same generators were used in the experiment, which is necessary for comparing the results with those of the LQR and MPC algorithms, the numerical values obtained in the identification phase were also identical [4]. In this study, after reducing the phase to a value below $\Delta\varphi$, we do not switch the control to a new algorithm but continue the synchronization process using the SMC.

In the initial phase, specifically when entering the synchronous state, the SMC algorithm effectively reduced the phase error to levels specified by the experimenter. For instance, the LPFRS-01 oscillator takes 46 s, the SMAC E10-MRX oscillator takes 47 s, and the miniature cesium CSAC SA.45s takes 18 s to decrease the initial phase error from 100 ns to under 10 ns. These differences are directly linked to the tuning range of each generator.

In MPC, we use only the values of the estimation $\hat{x}_{ph}(n)$ phase error, as is the case in many other VCO synchronization algorithms, for example, with a proportional-integral controller (PI). Even after using Kalman filtration, we will not meet most telecommunications standards. The SMC algorithm, which is based solely on phase measurement, produces oscillations with high dynamics near the sliding plane. An example of this behavior is shown in Figure 2. The signal directly from the phase detector is marked in green (plot P1), the blue color shows the phase error at the output of the Kalman filter (plot P2), and the red color indicates the output of the system in relation to the reference signal from the external standard used in the measurements (plot P3).

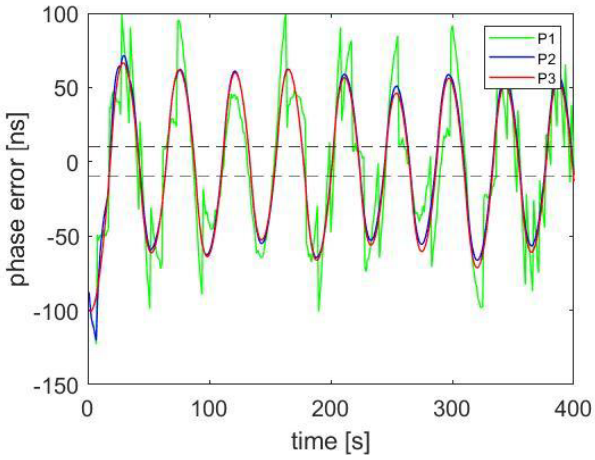

FIGURE 2. Time plot showing the process of synchronizing a CSAC SA.45s oscillator using a sliding control limited to phase difference measurement only; P1 – output of the phase detector, P2 – output of the Kalman filter, P3 - output of the system to the external reference.

The use of phase estimation and its derivative smooths out the output of the Kalman filter and the output of the system (Fig. 3) and, as we will show next, allows us to meet even the most demanding ITU-T recommendations for MTIE and TDEV for the PRC clock if the sliding control works with a Kalman filter.

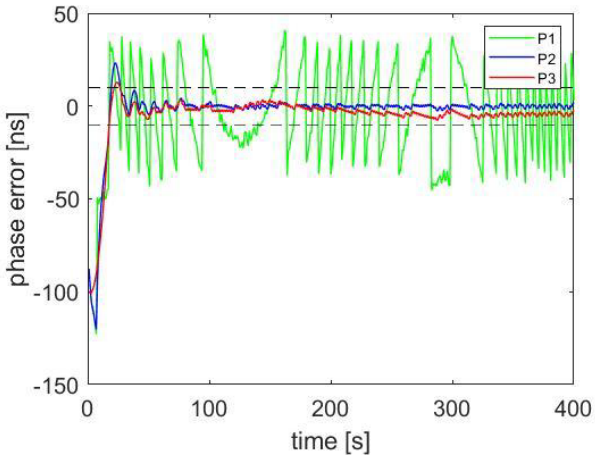

FIGURE 3. Time plot showing the process of synchronizing the CSAC SA.45s oscillator using the sliding control, exploiting both phase difference and its derivative; P1 – output of the phase detector, P2 – output of the Kalman filter, P3 - output of the system to the external reference.

Figure 4 shows the values of the MTIE, and Figure 5 shows the values of the TDEV for the three generators used during the experiments and the values of the PRTC B norm (ITU PRTC B).

Fig.s 4-5 show that using only sliding control to control the frequency of high-stability oscillators can be helpful in telecommunications, providing fast and high-quality synchronization to a 1 PPS signal. The PRTC B standard for the

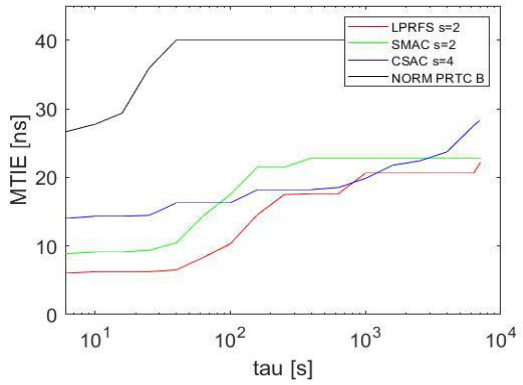

FIGURE 4. The MTIE values of the LPFRS-01, SMAC E10-MRX, and CSAC SA.45s oscillators for sliding mode control with parameter *s*.

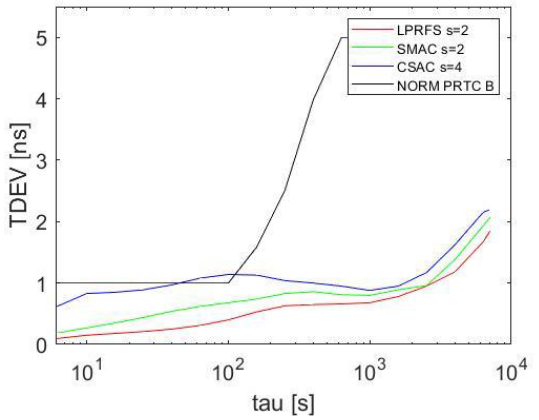

FIGURE 5. The TDEV values of the LPFRS-01, SMAC E10-MRX, and CSAC SA.45s oscillators for sliding mode control with parameter *s*.

MTIE was met with a large margin for all three generators. The value of divider s is the smallest value at which the norm is satisfied. For $\tau < 40$ s, differences in the short-term stability of the generators were clearly visible. For higher τ values, the differences between the generators were blurred. Note also that the PRTC B telecommunications standards on MTIE can be met even with the relatively wide tuning range of the local oscillator frequency offered by CSAC ($\pm 2.2 \cdot 10^{-8}$) and a properly selected divisor s.

The PRTC B standard for TDEV was met with a relatively small margin. For $\tau < 200$ s, the difference in the short-term stability of the oscillators was clearly visible. For larger τ, the differences in TDEV are blurred, which results from the long-term parameters of the 1 PPS signal. Unfortunately, the PRTC B standard was not met for the CSAC generator. This is because a controller cannot alter the fundamental physics of the oscillator itself. The control algorithm was designed to regulate the long-term behavior of an oscillator and reject external disturbances, providing a general approach applicable to any oscillator. At the same time, it should be remembered that this is still an excellent result, and less demanding standards, such as PRC, are being met.

When the algorithm is on the sliding plane, that is, in the vicinity of the zero phase, the minimum or maximum control voltage is alternately exposed, and the value of the codeword does not provide sufficient quality of sustain when switching to the HOLDOVER, that is, after the loss of the synchronizing signal of 1 PPS. An ideal transition is theoretically provided by a situation where both the phase difference $x_{ph}(n)$ and the rate of phase difference change $x_{dph}(n)$, are equal to zero. In practice, such a situation rarely occurs because the system is still subject to regulation, even in a steady state. After losing the reference signal, the system uses the control voltage as an average control value over the past K seconds. In our research, the value of $K = 10\,000$ gave satisfactory results for the relative initial frequency offset in the holdover state of the order 10^{-11}. Another factor is the long-term stability of the oscillator and the thermal changes in the system and its surroundings, which also affect the holdover quality. Recovery from the holdover state can also be performed using the SMC algorithm, as this solution provides the fastest correction of the phase error and ensures a high-quality steady-state synchronization.

For an oscillator with a tuning range of $\pm 2 \cdot 10^{-9}$ e.g., for SMAC E10-MRX, if we want to obtain an initial frequency error of less than 10^{-11} when going into holdover, the codeword error must be less than 0.5% of the entire adjustment range. Figure 6 shows the changes in the average codeword value for the SMAC E10-MRX oscillator during 12 h of observation. The final $K = 10\,000$ samples were averaged. The figure shows that the difference between the maximum and minimum values of the average codeword intended for holdover was less than 0.3% of the VCO frequency control range. This means that, at any time when we lose the signal, we are guaranteed an initial frequency detuning of less than 10^{-11}, as shown in Figure 6. A similar result is obtained for the LPFRS-01 oscillator, which results from a similar tuning range and identical s-value.

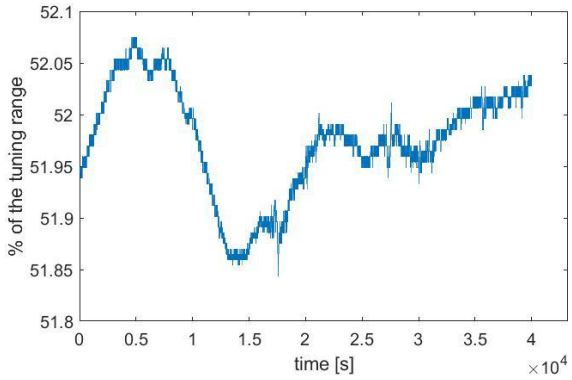

FIGURE 6. Change of the value of the HOLDOVER codeword for the SMAC E10-MRX oscillator (s=2) over 12 hours for the averaged last K=10 000 samples expressed as a percentage of the entire tuning range.

If we use the divisor $s = 4$ for the CSAC oscillator and average $K = 10000$ samples, the code word changes within

a width of less than 0.25% of the entire adjustment range (Fig. 7). Because the tuning range of the CSAC oscillator is $\pm 2.2 \cdot 10^{-8}$, the relative initial frequency error will be on the order of $\pm 5.5 \cdot 10^{-11}$.

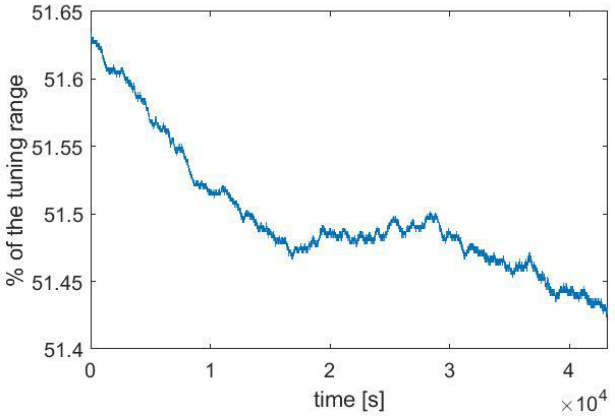

FIGURE 7. Change of the value of the HOLDOVER codeword for the CSAC SA.45s oscillator (s=4) over 12 hours for the averaged last K=10000 samples expressed as a percentage of the entire tuning range.

IV. SUMMARY AND CONCLUSION

This article describes the application of the SMC algorithm, derived from the theory of optimal control, for achieving frequency and phase synchronization in high-stability oscillators. It has been shown that SMC based on the simultaneous use of phase difference and the dynamics of changes in this difference leads to the fast achievement of synchronization and maintenance with satisfactory quality. The tests were conducted for three oscillator classes from various manufacturers. Sliding Mode Control provides a high-quality output signal that meets the telecommunication standards for MTIE and TDEV without implementing significantly more complex LQR or MPC algorithms. For all tested generators, the obtained MTIE values were considerably lower than the limit values contained in the requirements for the PRTC B clock [16]. The TDEV standard for the PRTC B clock is met for the LPFRS-01 and SMAC E10-MRX generators. In the case of the CSAC SA.45s oscillator, we observe slight exceedances of the norm for windows with a width of less than 200 s because of the worse short-term parameters of the CSAC oscillator. The MTIE and TDEV values did not change significantly after switching the generator to another unit of the same type and manufacturer. The observed differences in MTIE and TDEV values did not exceed 5 %, indicating a high reproducibility of the tuning characteristics of the VCOs used. The primary disadvantage of SMC is the significant initial frequency error that occurs when entering the holdover state after losing the 1 PPS signal. Therefore, it was proposed to supplement the SMC control with a procedure for entering the holdover state after the loss of the 1 PPS signal, which significantly reduces the initial frequency error of the local oscillator after switching to the holdover. Although the primary focus of the current study serves as a critical proof-of-concept, demonstrating the utility of the SMC method in fast phase and frequency synchronization of high-stability oscillators, the achieved results are directly applicable in telecommunications for a broad range of oscillators.

REFERENCES

[1] W. Guo, M. Zhu, S. Gu, H. Zuo, and J. Liu, "Linear quadratic Gaussian-based clock steering system for GNSS real-time precise point positioning timing receiver," *GPS Solutions*, vol. 28, no. 1, p. 53, Jan. 2024.

[2] K. Liu, X. Guan, X. Ren, and J. Wu, "Disciplining a Rubidium atomic clock based on adaptive Kalman filter," *Sensors*, vol. 24, no. 14, p. 4495, Jul. 2024.

[3] C. Dalmazzone, M. Guigue, L. Mellet, B. Popov, S. Russo, V. Voisin, M. Abgrall, B. Chupin, C. B. Lim, P.-É. Pottie, and P. Ulrich, "Precise synchronization of a free-running Rubidium atomic clock with GPS time for applications in experimental particle physics," *Nucl. Instrum. Methods Phys. Res. A, Accel. Spectrom. Detect. Assoc. Equip.*, vol. 1075, Jun. 2025, Art. no. 170358.

[4] P. Kubczak, M. Jessa, and M. Kasznia, "Fast frequency and phase synchronization of high-stability oscillators with 1 PPS signal from satellite navigation systems," *GPS Solutions*, vol. 29, no. 1, pp. 52-1–52-18, Jan. 2025.

[5] L. S. Pontryagin, V. Boltayanskii, R. V. Gamkrelidze, and E. F. Mishchenko, *The Mathematical Theory of Optimal Processes*. Hoboken, NJ, USA: Wiley, 1962.

[6] K. G. Mishagin, V. A. Lysenko, and S. Y. Medvedev, "A practical approach to optimal control problem for atomic clocks," *IEEE Trans. Ultrason., Ferroelectr., Freq. Control*, vol. 67, no. 5, pp. 1080–1087, May 2020.

[7] P. Wolfrum, R. L. Scheiterer, and D. Obradovic, "An optimal control approach to clock synchronization," in *Proc. IEEE Int. Symp. Precis. Clock Synchronization Meas., Control Commun.*, Portsmouth, NH, USA, Sep. 2010, pp. 122–128.

[8] T. D. Schmidt, M. Gödel, and J. Furthner, "Investigation of pole placement technique for clock steering," in *Proc. Precise Time Time Interval Syst. Appl. Meeting*, Feb. 2018, pp. 22–29.

[9] P. Koppang and R. Leland, "Linear quadratic stochastic control of atomic hydrogen masers," *IEEE Trans. Ultrason., Ferroelectr., Freq. Control*, vol. 46, no. 3, pp. 517–522, May 1999.

[10] V. Utkin, "Variable structure systems with sliding modes," *IEEE Trans. Autom. Control*, vol. AC-22, no. 2, pp. 212–222, Feb. 1977.

[11] M. T. Vu, S. H. Kim, D. H. Pham, H. L. N. N. Thanh, V. H. Pham, and M. Roohi, "Adaptive dynamic programming-based intelligent finite-time flexible SMC for stabilizing fractional-order four-wing chaotic systems," *Mathematics*, vol. 13, no. 13, p. 2078, Jun. 2025.

[12] M. Roohi, S. Mirzajani, A. R. Haghighi, and A. Basse-O'Connor, "Robust design of two-level non-integer SMC based on deep soft actor-critic for synchronization of chaotic fractional order memristive neural networks," *Fractal Fractional*, vol. 8, no. 9, p. 548, Sep. 2024.

[13] M. Roohi, S. Mirzajani, A. R. Haghighi, and A. Basse-O'connor, "Robust stabilization of fractional-order hybrid optical system using a single-input TS-fuzzy sliding mode control strategy with input nonlinearities," *AIMS Math.*, vol. 9, no. 9, pp. 25879–25907, 2024.

[14] S. Jamshidi, A. Safa, and S. Mirzajani, "Continuous nonsingular fast terminal sliding mode control for a free gyro stabilized mirror system," *IEEE Trans. Autom. Sci. Eng.*, vol. 22, pp. 10937–10947, 2025.

[15] H. Kizmaz, "Comparative analysis of optimal control strategies: LQR, PID, and sliding mode control for DC motor position performance," *Gazi Univ. J. Sci. A, Eng. Innov.*, vol. 10, no. 4, pp. 571–592, Dec. 2023.

[16] ITU-T. (Nov. 2018). *ITU G.8272*. Accessed: Oct. 31, 2025. [Online]. Available: https://www.itu.int/rec/t-rec-g.8272/en

[17] J.-J. Lee and Y. Xu, "A multiple-rate control scheme of robot manipulators," *J. Syst. Eng.*, vol. 1, pp. 22–33, May 1993.

[18] P. Benner, "Solving large-scale control problems," *IEEE Control Syst. Mag.*, vol. 24, no. 1, pp. 44–59, Jan. 2004.

[19] A. Bemporad, "Model predictive control design: New trends and tools," in *Proc. 45th IEEE Conf. Decis. Control*, Dec. 2006, pp. 6678–6683.

[20] L. Galleani, "Time-frequency analysis of atomic clock anomalies," in *Proc. Eur. Freq. Time Forum (EFTF)*, Apr. 2018, pp. 281–284.

[21] A. Cernigliaro, G. Fantino, I. Sesia, P. Tavella, and L. Galleani, "Nonstationarities in space clocks: Investigations on experimental data," in *Proc. Eur. Freq. Time Forum (EFTF)*, Jun. 2014, pp. 126–129.

[22] P. Kubczak, J. Nikonowicz, and L. Matuszewski, "Kalman filter design for fast synchronization of a high-stability Rubidium oscillator," in *Proc. Signal Process., Algorithms, Archit., Arrangements, Appl. (SPA)*, Sep. 2019, pp. 77–80.
[23] P. Kubczak, M. Kasznia, and M. Jessa, "Preprocessing for fast synchronization of high-stability oscillators disciplined by GNSS 1 PPS signal," in *Proc. Eur. Freq. Time Forum (EFTF)*, Apr. 2018, pp. 234–239.
[24] S. K. Nanda, G. Kumar, V. Bhatia, and A. K. Singh, "Kalman filtering with delayed measurements in non-Gaussian environments," *IEEE Access*, vol. 9, pp. 123231–123244, 2021.
[25] J. K. Pieper, "First order dynamic sliding mode control," in *Proc. 37th IEEE Conf. Decis. Control*, vol. 3, Tampa, FL, USA, Mar. 1998, pp. 2415–2420.
[26] V. Boltyanskii, *Mathematical Methods of Optimal Control*. New York, NY, USA: Holt, Rinehart and Winston, 1971.
[27] S. W. Smith, "Moving average filters," in *Digital Signal Processing*. Boston, MA, USA: Newnes, 2003, ch. 15, pp. 277–284.

PAWEŁ KUBCZAK received the M.S. degree from Poznań University of Technology, in 2013. He continues his studies at the Faculty of Electronics and Telecommunications and is currently preparing his Ph.D. thesis. His research interests include phase-locked loops and network synchronization, digital measurement systems, time interval error measurement, randomness in digital logic, microcontrollers, and field programmable gate arrays.

MIECZYSŁAW JESSA was born in Poland, in 1961. He received the M.Sc.Eng. (Hons.) and Ph.D. degrees from Poznań University of Technology, in 1985 and 1992, respectively. Since 2017, he has held the position of a Professor at the Institute of Multimedia Telecommunications, Faculty of Computing and Telecommunications, Poznań University of Technology. He is currently the author or co-author of over 150 journal and conference papers and 15 patents. His research interests include phase-locked loops, network synchronization, and the mathematical models of randomness and pseudo-randomness.

JAKUB NIKONOWICZ (Senior Member, IEEE) received the M.Sc. and Ph.D. degrees in telecommunications from Poznań University of Technology, in 2014 and 2019, respectively. Since 2019, he has held the position of an Assistant Professor at the Institute of Multimedia Telecommunications, Faculty of Computing and Telecommunications, Poznań University of Technology. He has authored or co-authored over a dozen scientific publications in refereed journals and proceedings of international conferences. Additionally, he was the Project Manager for grants supporting young scientists and as the Co-Principal Investigator in an international research consortium. His current research interests include innovations in statistical signal processing for next-generation communication and security technologies.